JOURNAL OF PHYSICAL ORGANIC CHEMISTRY
J. Phys. Org. Chem. 2005; **18:** 462–467
Published online 5 October 2004 in Wiley InterScience (www.interscience.wiley.com). DOI: 10.1002/poc.871

DFT calculations on the allenyl Cope rearrangement of *syn*-7-allenylnorbornene: comparison with results obtained from CASSCF calculations

James A. Duncan* and Marie C. Spong†

Department of Chemistry, Lewis and Clark College, Portland, Oregon 97219-7899, USA

Received 4 August 2004; accepted 9 August 2004

ABSTRACT: The conformationally restricted allenyl Cope rearrangement of *syn*-7-allenylnorbornene (**10**) to racemic-triene **11** was studied computationally using density functional theory (DFT) methods and the results were compared with those already calculated for this rearrangement at the (8,8)CASPT2/6–31G*//(8,8)CASSCF/6–31G* level of theory. The CASSCF level calculations had shown that the rearrangement involves two separate transition structures **12** and **13** that both lead to common diradical intermediate **14**. These findings are consistent with the 90% stereoselectivity observed in the thermal Cope rearrangements of dimethyl allenylnorbornene derivatives racemic **7a** and **7b**. In this study, we found that CASSCF optimized structures **10**–**12** and **15** could be successfully re-optimized at the UB3LYP/6–31G* level to structures of similar geometries and relative enthalpies. However, the CASSCF transition structure corresponding to **13** did not optimize to a UB3LYP version of **13**, but rather to the UB3LYP-optimized structure corresponding to transition structure **12**. Despite taking several approaches, an optimized UB3LYP/6–31G* version of **13** was not found on the UB3LYP potential energy surface. Hence the UB3LYP results are not only at variance with the CASSCF results but also with the above mentioned experimental results. The **10** → **11** rearrangement was also studied using UBLYP and UBPW91 functionals in addition to UB3LYP and each of the three functionals predicted a different mechanism, none of them consistent with the experimental or CASSCF results. Copyright © 2004 John Wiley & Sons, Ltd.
Supplementary electronic material for this paper is available in Wiley Interscience at http://www.interscience.wiley.com/jpages/0894-3230/suppmat/

KEYWORDS: theoretical calculations; allenylnorbornene; Cope reaction mechanism; density functional theory; CASSCF

INTRODUCTION

The thermal Cope rearrangement has been the subject of numerous experimental and computational studies.[1] For example, multireference (6,6)CASSCF/6–31G* level calculations on the paradigmatic Cope rearrangement of 1,5-hexadiene, that included dynamic electron correlation using either CASPT2[2] or CASMP2[3] versions of multi-reference perturbation theory, have shown that it proceeds by way of a concerted reaction.[1g,1h]

Excellent results have also been obtained using density functional theory (DFT) calculations, performed with the B3LYP functional (this is the hybrid, Becke, three-parameter, exchange functional of Lee, Yang, and Parr[4]), for the concerted Cope rearrangements of 1,5-hexadiene[1i,1j] and more highly unsaturated derivatives.[1k] The aromatic character of certain of these concerted transition structures has also been confirmed by computed magnetic properties[5] and the density of effectively unpaired electrons.[6]

Some Cope rearrangements, however, have been found to be non-concerted. For example, radical stabilizing groups[7] or relief of steric strain[5b,8] have resulted in mechanisms in which bond breaking precedes bond making, resulting in bis-allyl diradical intermediates. Cyclohexane-1,4-diyl derivatives have also been favored as intermediates for cases in which bond making precedes bond breaking.[9] Since both of these types of non-concerted Cope rearrangements involve singlet diradical intermediates, it might be expected that single reference DFT theory may have difficulty in dealing properly with them. Proper treatment would require that the reference wavefunction be represented by more than one Slater determinant and UDFT (unrestricted variant of DFT) calculations use single determinants of Kohn–Sham orbitals.[10]

It has also been reported that pure density functionals such as UBLYP and UBPW91 perform better than hybrid functionals (e.g. B3LYP) for certain reactions involving singlet diradical intermediates. Schreiner has reported that UBLYP performs much better than UB3LYP in calculations on dehydrobenzene singlet diradicals as

**Correspondence to:* J. A. Duncan, Department of Chemistry, Lewis and Clark College, Portland, Oregon 97219-7899, USA.
E-mail: duncan@lclark.edu
†Present address: Department of Chemistry and Chemical Biology, Harvard University, 12 Oxford Street, Cambridge, Massachusetts 02138, USA.
Contract/grant sponsor: National Science Foundation; *Contract/grant number:* DUE-9750586.

intermediates in the Bergman cyclization of enediynes.[11] In addition, calculations performed by Staroverov and Davidson on the Cope rearrangements of 1,3,5-tricyano-1,5-hexadiene and 1,3,4,6-tetracyano-1,5-hexadiene have shown that UBPW91 gives much more believable results than either UB3LYP or UB3PW91, with the last two methods predicting what the authors consider a spurious stationary point in each case.[6]

Another reaction that has been studied recently, by both experimental and theoretical methods, is the *allenyl* Cope rearrangement of 1,2,6-heptatriene (**1**) to methylene-1,5-hexadiene (**2**). Roth *et al.* have shown that approximately half of this rearrangement proceeds through a trappable monoallylic cyclohexane-1,4-diyl diradical intermediate **3**.[12] Wessel and Berson have also studied the allenyl Cope rearrangement of (*R*,*E*)-5-methyl-1,2,6-octatriene (**4**), an optically active dimethyl derivative of **1**.[13] Based on the observed stereochemistry of this reaction, which affords all four possible configurational stereoisomers of 4-methyl-3-methylene-1,5-heptatriene (**5**), they concluded that at least 16% of the rearrangement passes through configurationally diastereomeric diradicals **6**.

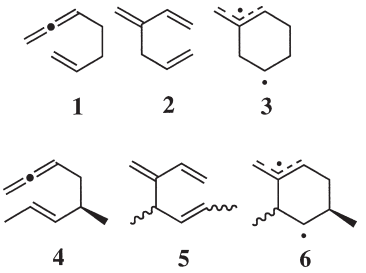

1 **2** **3**

4 **5** **6**

The **1** → **2** rearrangement was subsequently studied by computational methods.[14] Both (8,8)CASPT2/6–31G*//(8,8)CASSCF/6–31G* and UB3LYP/6–31G* calculations gave very similar descriptions of the potential energy surface (PES), finding two different pathways that diverge only after passage over a common rate-determining transition state. One pathway leads to formation of diradical **3** whereas the other leads directly to product **2**, without formation of intermediate **3**. Furthermore, neither of the calculated transition structures (i.e. between **1** and **3** and between **2** and **3**) exhibited appreciable allylic delocalization. For this particular Cope rearrangement, the less costly UB3LYP calculation was shown to perform as well as the more costly CASSCF calculation, even though it involves, in part, a singlet diradical intermediate.

One of us has also made an experimental study of the *conformationally restricted* allenyl Cope rearrangement of dimethyl *syn*-7-allenylnorbornenes racemic **7a** and racemic **7b**.[15] The reaction was found to be essentially 90% stereoselective. Pyrolysis of epimer **7a** gave 95% of a mixture of (*E*)-**8** and (*Z*)-**9** and 5% of a mixture of (*Z*)-**8** and (*E*)-**9**. Correspondingly, pyrolysis of the other epimer (**7b**) gave 96% of a mixture of (*Z*)-**8** and (*E*)-**9** and 4% of a mixture of (*E*)-**8** and (*Z*)-**9**.

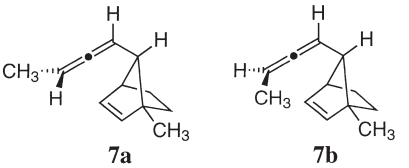

7a **7b**

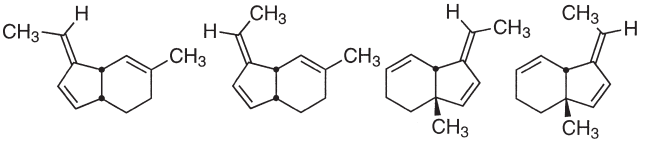

(*E*)-**8** (*Z*)-**8** (*E*)-**9** (*Z*)-**9**

Although a concerted mechanism might explain the formation of the major products from both **7a** and **7b**, it cannot, by itself, account for the formation of the minor products. Therefore, we concluded that a monoallylic bicyclic 1,4-diyl intermediate was involved in the reaction, *at least* in the formation of the minor products.

In an attempt to account for the stereoselectivity observed in the **7** → **8** + **9** rearrangements, we subsequently performed calculations at the (8,8)CASPT2/6–31G*//(8,8)CASSCF/6–31G* level of theory on the Cope rearrangement of *syn*-7-allenylnorbornene (**10**) to give racemic trienes **11**.[16] The calculations indicated that the **10** → **11** rearrangement is much more complicated than similar CASSCF calculations made the **1** → **2** rearrangement out to be. As mentioned above for the **1** → **2** rearrangement, two possible pathways involving a single rate-determining transition structure were found, one a **1** → **3** → **2** non-concerted pathway and the other a **1** → **2** concerted pathway. By contrast, for the **10** → **11** rearrangement the PES was calculated to involve two separate rate-determining transition structures **12** and **13**, which both lead to the common diradical intermediate **14**. Optimized structures for **12** and **13** are shown in Fig. 1. Transition structure **13**, which has virtually zero allylic stabilization, was found to be 2.1 kcal mol^{-1} (1 kcal = 4.184 kJ) higher in enthalpy than **12** and a common lower energy transition structure **15** was found to connect diradical **14** and product **11**. The terminal methylene group of **10** was also shown to rotate in only one direction when passing through transition structure **12** ('stereospecific' pathway), but to rotate freely in either direction when passing through transition structure **13** (non-'stereospecific' pathway).

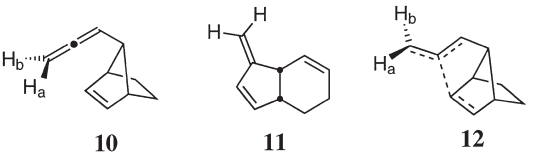

10 **11** **12**

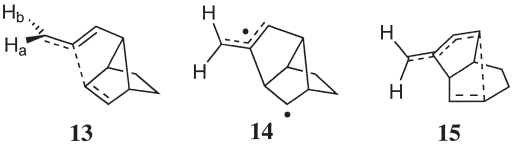

13 **14** **15**

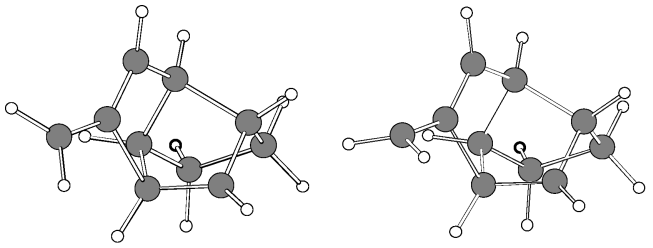

12 **13**

Figure 1. CASSCF/6–31G* optimized geometries of transition structures **12** and **13**. Coordinates can be found in the Supporting Information section of Ref. 16

If the **7** → **8** + **9** rearrangement proceeds in a similar manner to the **10** → **11** rearrangement, the formation of the major products **8** and **9** from **7** could be interpreted in terms of a comparable 'stereospecific' **10** → **12** → **14** → **15** → **11** pathway, whereas the formation of the minor products could be seen as arising from the comparable non-'stereospecific' **10** → **13** → **14** → **15** → **11** pathway.

CASSCF calculations have thus been shown to give excellent agreement with experiment for both the **1** → **2** and **10** → **11** allenyl Cope rearrangements. As UB3LYP calculations also gave good results for the **1** → **2** rearrangement, in spite of the perceived shortcomings of the method for reactions involving singlet diradical intermediates,[10] we were anxious to test the performance of UB3LYP on the apparently more complex **10** → **11** rearrangement. We were particularly interested to see if UB3LYP would reproduce both the **10** → **12** → **14** → **15** → **11** ('stereospecific') and **10** → **13** → **14** → **15** → **11** (non-'stereospecific') pathways uncovered by the CASSCF calculations.

The current popularity of the B3LYP functional for DFT calculations also served as an impetus to make it the focus of our DFT study. However, in view of recent reports that B-functionals might be more appropriate than B3-functionals for a study of the Cope and related rearrangements,[6,11] we were also interested in making some comparisons of the two functional types in our DFT study of the **10** → **11** rearrangement.

COMPUTATIONAL METHODOLOGY

The majority of the UDFT calculations (unrestricted variant of DFT) were carried out using the hybrid Becke three-parameter exchange functional of Lee, Yang, and Parr[4b] (UB3LYP). Other calculations were done using the UBLYP and UBPW91 functionals. All calculations made use of the 6–31G* basis set and the Gaussian 94[17a] or Gaussian 98[17b] suite of programs. The structures resulting from these calculations are represented approximately by ChemDraw structures in Table 1 and their

Table 1. Carbon–carbon bond lengths (Å) for stationary points on the (8,8)CASSCF,[16] UB3LYP, UBLYP and UBPW91 potential surfaces for the Cope rearrangement of *syn*-7-allenylnorbornene (**10**) to triene **11** (**10**–**16**), obtained with the 6–31G* basis set[a]

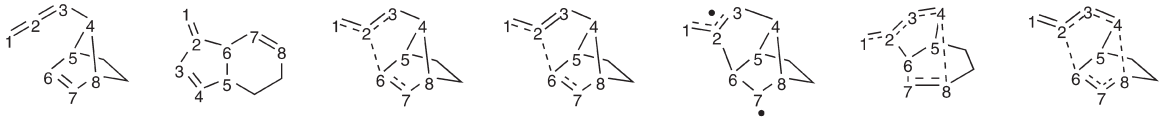

10 **11** **12** **13** **14** **15** **16**

Structure	Method	C_1—C_2	C_2—C_3	C_3—C_4	C_4—C_5	C_5—C_6	C_6—C_7	C_7—C_8	C_4—C_8	C_2—C_6
10	CASSCF	1.32	1.32	1.51	1.55	1.52	1.34	1.52	1.58	
	RB3LYP	1.31	1.31	1.51	1.56	1.52	1.34	1.52	1.56	
	RBLYP	1.32	1.32	1.52	1.58	1.53	1.35	1.53	1.58	
	RBPW91	1.32	1.32	1.51	1.57	1.52	1.35	1.52	1.57	
11	CASSCF	1.34	1.47	1.34	1.52	1.55	1.51	1.34		1.56
	RB3LYP	1.34	1.46	1.34	1.51	1.56	1.52	1.34		1.54
	RBLYP	1.35	1.47	1.35	1.52	1.58	1.53	1.35		1.55
12	CASSCF	1.37	1.36	1.49	1.54	1.54	1.43	1.50	1.63	1.90
	UB3LYP	1.35	1.36	1.48	1.55	1.55	1.42	1.49	1.63	1.88
13	CASSCF	1.41	1.34	1.51	1.54	1.54	1.44	1.51	1.60	1.84
14	CASSCF	1.37	1.41	1.50	1.55	1.55	1.52	1.52	1.61	1.57
	UB3LYP	1.37	1.41	1.50	1.56	1.57	1.52	1.51	1.59	1.54
	UBPW91	1.38	1.41	1.50	1.57	1.57	1.52	1.51	1.60	1.55
15	CASSCF	1.36	1.43	1.44	1.54	1.55	1.52	1.46	1.90	1.58
	UB3LYP	1.36	1.43	1.43	1.54	1.56	1.52	1.44	1.93	1.55
16	RB3LYP	1.34	1.38	1.44	1.54	1.55	1.42	1.45	1.80	1.83
	RBLYP	1.35	1.39	1.45	1.56	1.57	1.43	1.46	1.81	1.86
	RBPW91	1.36	1.38	1.46	1.55	1.56	1.43	1.47	1.71	1.81

[a] The RB3LYP structure **16** is a second-order saddle point, exhibiting two imaginary frequencies. Full sets of coordinates and energies for all B3LYP, BLYP and BPW91 structures are available in the Supplementary materials. Coordinates and energies for all CASSCF structures are available in the Supporting Information accompanying Ref. 16.

coordinates, energies, spin contamination values (S^2), and imaginary frequencies are provided in the Supplementary material (available in Wiley Interscience). When UB3LYP, UBLYP, and UBPW91 wavefunctions reduced to their restricted variant (i.e. when $S^2 = 0$), they are represented in Table 1, and below, as RB3LYP, RBLYP and RBPW91 wavefunctions, respectively. Appropriate vibrational analyses were also carried out to characterize stationary points as energy minima or as transition structures and to obtain zero-point energy differences. All energy comparisons that follow are between zero-point energy corrected structures.

RESULTS AND DISCUSSION

Since (8,8)CASSCF optimized versions of structures **10**–**15** were available from previous calculations,[16] our first series of calculations consisted of re-optimizing them at the UB3LYP level. As shown in Table 1, (8,8)CASSCF-optimized structures **10**–**12**, **14** and **15** were successfully re-optimized at the UB3LYP level to structures of similar geometries. Figure 2 compares the relative enthalpies among these structures calculated at the (8,8)CASPT2/6–31G*//(8,8)CAACF/6–31G* and UB3LYP/6–31* levels of theory. The agreement is reasonably good, although it is less so when the energies of **12** ($S^2 = 0.386$), **14** ($S^2 = 1.031$) and **15** ($S^2 = 0.751$) were corrected for spin contamination. {Corrections were made using the following equation, where labels 1 and 3 refer to singlet and triplet, respectively: $E1\ (\text{corr}) = E1\ (\text{UDFT}) + [(<S^2>1/(<S^2> 3 - <S^2>1)] \times [E1(\text{UDFT}) - E3(\text{UDFT})]$.[18] Connections among all structures on the UB3LYP and CASSCF[16] potential energy surfaces were confirmed by intrinsic reaction coordinate (IRC) calculations. Thus

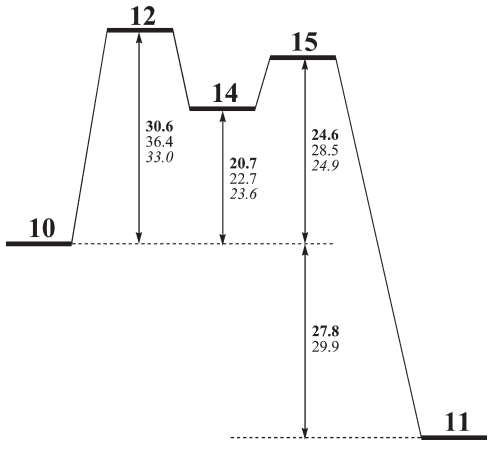

Figure 2. Reaction coordinate diagram showing zero-point corrected enthalpy differences (in kcal mol^{-1}) among optimized structures **10**–**12**, **14** and **15**, computed at the (8,8)CASPT2/6–31G*//(8,8)CASSCF/6–31G* (bold type)[16] and UB3LYP/6–31G* (normal type) levels of theory. UB3LYP/6–31G* energies further corrected for spin contamination are shown in italics

UB3LYP calculations reproduce well the **10** → **12** → **14** → **15** → **11** 'stereospecific' pathway uncovered earlier using (8,8)CASSCF calculations.

Importantly, however, UB3LYP optimization of (8,8)CASSCF-optimized transition structure **13** did not produce a UB3LYP version of structure **13** but rather the UB3LYP-optimized structure corresponding to transition structure **12**. (8,8)CASSCF-optimized **13** had been obtained previously[16] by employing a Synchronous Transit-Guided Quasi-Newton (STQN) calculation using (8,8)CASSCF-optimized **10** and **11** as the starting structures. [This calculation was done in the search for a possible concerted transition structure between **10** and **11**. However, the first-order saddle point obtained (**13**) was shown by IRC calculations to connect to diradical **14** (in addition to **10**) and not to product **11**[16]]. However, when a similar STQN calculation was performed at the UB3LYP level using UB3LYP-optimized **10** and **11** as starting structures, the resulting structure **16** (cf. Table 1) resembled a concerted transition state (i.e. relatively long C_2—C_6 and C_4—C_8 bonds) but had two imaginary frequencies. [Animation of one imaginary frequency ($-763\,\text{cm}^{-1}$) stretched only the C_2—C_6 bond whereas animation of the other ($-416\,\text{cm}^{-1}$) stretched only the C_4—C_8 bond (cf. Table 1)]. Hence it appears that a transition structure resembling **13**, i.e. with virtually zero allylic stabilization, does not exist on the UB3LYP PES and hence the non-'stereospecific' **10** → **13** → **14** → **15** → **11** pathway is not readily reproduced using UB3LYP. [When a single-point energy calculation was performed at the UB3LYP level on transition structure **13**, using its (8,8)CASSCF-optimized geometry, the resulting structure had an enthalpy 2.9 kcal mol^{-1} higher than the UB3LYP transition structure **12**. This compares with a 2.1 kcal mol^{-1} enthalpy difference between (8,8)CASSCF-optimized structures **12** and **13**].

Next we investigated whether the **10** → **12** → **14** → **15** → **11** pathway could be obtained using UB3LYP calculations alone, i.e. without reference to the CASSCF-optimized structures as discussed above. (8,8)CASSCF-optimized structures **12** and **15** had been obtained by incrementally lengthening the C_2—C_6 or C_4—C_8 bonds in diradical **14** (cf. Table 1) that must be cleaved to produce reactant **10** or product **11**, respectively, with optimization at each step.[16] The highest energy structures thus obtained were then successfully optimized as first-order saddle points (**12** and **15**) at the (8,8)CASSCF/6–31G* level. When a UB3LYP calculation, beginning from the UB3LYP-optimized diradical **14**, was conducted in exactly the same way, a UB3LYP version of transition structure **15** was readily obtained on the product (**11**) side. On the reactant (**10**) side, however, optimization of the highest point obtained at the UB3LYP level did not produce UB3LYP-optimized **12**, but rather structure **16** (cf. Table 1) with two imaginary frequencies. [Even when a very small step size (0.01 bohr) and the 'notrustupdate' keyword in Gaussian 98 were used for the

transition structure optimization, the resulting structure was **16** and not structure **12**]. However, optimization of the structure of slightly lower energy on the side towards the diradical did produce the same UB3LYP structure **12** that was produced from UB3LYP/6–31G* optimization of the CASSCF version of **12** as starting structure. Thus, although the $\mathbf{10} \rightarrow \mathbf{12} \rightarrow \mathbf{14} \rightarrow \mathbf{15} \rightarrow \mathbf{11}$ pathway was eventually found using UB3LYP calculations alone, transition structure **12** was not uncovered in a straightforward manner.

On the other hand, optimization of (8,8)CASSCF-optimized transition structure **13** at the UBLYP level gave a structure resembling **16** with only one imaginary frequency ($-494\,\mathrm{cm}^{-1}$). Animation of this imaginary frequency simultaneously stretched both the C_2—C_6 and C_4—C_8 bonds (cf. Table 1) and IRC calculations confirmed that the RBLYP-optimized transition structure **16** connects to reactant **10** and product **11** on the RBLYP PES. The calculated enthalpy difference between RBLYP reactant **10** and transition structure **16** is 33.1 kcal mol^{-1}. This is 2.5 kcal mol^{-1} higher than the (8,8)CASPT2/6–31G*//(8,8)CASSCF/6–31G* enthalpy difference between reactant **10** and transition structure **12** and 0.1 kcal mol^{-1} higher than the UB3LYP enthalpy difference (after correction for spin contamination[18]) between **10** and **12** (cf. Fig. 2) [A UBLYP single-point calculation was also performed on UB3LYP structure **12** and the enthalpy difference between the resultant structure and RBLYP reactant **10** was calculated to be 34.8 kcal mol^{-1}; this value is close to the 33.1 kcal mol^{-1} enthalpy difference between RBLYP structures **16** (cf. Fig. 2) (the concerted transition structure) and RBLYP reactant **10**]. Given that the $\mathbf{7} \rightarrow \mathbf{8} + \mathbf{9}$ rearrangement has been shown experimentally not to involve a single concerted transition state,[15] it is unlikely that the RBLYP concerted transition structure **16** is a valid one.

Optimization of (8,8)CASSCF-optimized transition structure **13** at the UBPW91 level also gave a structure most closely resembling **16** with only one imaginary frequency ($-380\,\mathrm{cm}^{-1}$). As shown in Table 1, although the C_2—C_6 bond is lengthened to 1.81 Å, almost as much as it is in the corresponding RBLYP transition structure (1.86 Å), the C_4—C_8 bond is lengthened to 1.71 Å, only about half as much as in the the RBLYP case (1.81 Å). Furthermore, animation of the imaginary frequency primarily stretched the C_2—C_6 bond and IRC calculations showed that the RBPW91-optimized transition structure **16** is actually connected to diradical **14**, instead of product **11** (in addition to reactant **10**) on the UBPW91 PES. In addition, the terminal methylene group of **10** was found by this RBPW91 calculation to rotate in one direction only for the $\mathbf{10} \rightarrow \mathbf{16} \rightarrow \mathbf{14}$ process (A pathway from **14** to **11** was not calculated using the BPW91 functional). Based on this 'stereospecific' formation of diradical **14** using BPW91, one would expect the comparable $\mathbf{7} \rightarrow \mathbf{8} + \mathbf{9}$ rearrangements to give only the major products observed experimentally, i.e. (*E*)-**8** and (*Z*)-**9** from **7a** and (*Z*)-**8** and (*E*)-**9** from **7b**, with none of the minor products.[15]

CONCLUSIONS

We have found that the lower energy 'stereospecific' $\mathbf{10} \rightarrow \mathbf{12} \rightarrow \mathbf{14} \rightarrow \mathbf{15} \rightarrow \mathbf{11}$ pathway previously calculated[16] at the (8,8)CASPT2//(8,8)CASSCF level of theory can be well reproduced at the UB3LYP level (cf. Fig. 2). However, the slightly higher energy non-'stereoselective' $\mathbf{10} \rightarrow \mathbf{13} \rightarrow \mathbf{14} \rightarrow \mathbf{15} \rightarrow \mathbf{11}$ pathway appears not to exist on the UB3LYP PES: while a transition structure corresponding to **13**, with virtually zero allylic stabilization, was readily found at the (8,8)CASSCF level, such a structure could not be located by a similar method on the UB3LYP PES. Furthermore, even when the (8,8)CASSCF/6–31G* version of **13** is used as a starting structure for a UB3LYP/6–31G* optimization, the resulting transition structure is **12**, with a significant amount of allylic stabilization.

Hence the UB3LYP results appear to predict that the $\mathbf{10} \rightarrow \mathbf{11}$ rearrangement should be 100% 'stereospecific' via the $\mathbf{10} \rightarrow \mathbf{12} \rightarrow \mathbf{14} \rightarrow \mathbf{15} \rightarrow \mathbf{11}$ pathway, whereas the (8,8)CASSCF results produce an additional transition structure (**13**) that can account for the formation of the minor products in the Cope rearrangements of **7a** and **7b**, observed experimentally to be 90% stereoselective.[15] (Were it not for the fact that the CASSCF results are clearly in better agreement with the experimental results for the $\mathbf{7} \rightarrow \mathbf{8} + \mathbf{9}$ rearrangement,[15] it could be argued that the B3LYP calculations, which fail to locate transition structure **13**, are more correct than the CASSCF calculations; this is because the CASSCF method can exaggerate the stability of the diradical nature of transition structures and intermediates in some cases). Furthermore, the BLYP and BPW91 functionals were found to give results even more at variance with the (8,8)CASSCF calculated values,[16] and also with the experimental results obtained for the $\mathbf{7} \rightarrow \mathbf{8} + \mathbf{9}$ rearrangement.[15] The BLYP calculations predict only a single concerted $\mathbf{10} \rightarrow \mathbf{11}$ rearrangement and the BPW91 calculations a 'stereospecific' formation of diradical **14** and therefore product **11**. Moreover, the geometry of the BPW91-calculated transition structure (**16**) between reactant **10** and diradical **14** is very different from the geometries of transition structure **12**, which also links **10** to **14**, calculated at both the (8,8)CASSCF and UB3LYP levels (cf. C_4—C_8 and C_2—C_6 bond lengths in Table 1). [The UBPW91 enthalpy difference between **10** and **14** is 2.9 kcal mol^{-1} higher than the (8,8)CASPT2/6–31G*//(8,8)CASSCF/6–31G* enthalpy difference and 0.7 kcal mol^{-1} higher than the UB3LYP difference, after corrections for spin contamination[18]].

We compared the results of several calculations aimed at defining the PES for the apparently rather complex allenyl Cope rearrangement of *syn*-7-allenylnorbornene

(**10**) to triene **11** and found only the CASSCF results to be consistent with the stereoselectivity observed experimentally in the comparable allenyl Cope rearrangement of dimethyl-substituted allenylnorbornenes **7a** and **7b**.[15] Although computationally less expensive DFT calculations have given results commensurate with CASSCF for certain Cope rearrangements,[1i–k] that does not appear to be the case for the **10** → **11** rearrangement. Those doing their own calculations on Cope or similar rearrangements may want to take the results of our study into account in deciding upon the level and type of computational method or methods to employ. In this case, the CASSCF results appear to be superior to the B3LYP results.

Acknowledgements

We are grateful to the National Science Foundation (grant DUE-9750586) for providing funds for the purchase of several Silicon Graphics workstations used in the computations. We are especially indebted to Mr Brian Arthur for his technical assistance as System Administrator. We also thank Professor Stephen Tufte, of the Lewis and Clark College Physics Department, for the use of a R12000 Silicon Graphics workstation.

REFERENCES

1. (a) Borden WT, Loncharich RJ, Houk KN. *Annu. Rev. Phys. Chem.* 1988; **39**: 213–236; (b) Houk KN, Li Y, Evanseck JD. *Angew. Chem. Int. Ed. Engl.* 1992; **31**: 682–708; (c) Houk KN, Gonzalez J, Li Y. *Acc. Chem. Res.* 1995; **28**: 81–90; (d) Osamura Y, Kato S, Morokuma K, Feller D, Davidson ER, Borden WT. *J. Am. Chem. Soc.* 1984; **106**: 3362–3363; (e) Morokuma K, Borden WT, Hrovat DA. *J. Am. Chem. Soc.* 1988; **110**: 4474–4475; (f) Dupuis M, Murray C, Davidson ER. *J. Am. Chem. Soc.* 1991; **113**: 9756–9759; (g) Hrovat DA, Morokuma K, Borden WT. *J. Am. Chem. Soc.* 1994; **116**: 1072–1076; (h) Kozlowski PM, Dupuis M, Davidson ER. *J. Am. Chem. Soc.* 1995; **117**: 774–778; (i) Weist O, Black KA, Houk KN. *J. Am. Chem. Soc.* 1994; **116**: 10336–10337; (j) Jiao H, Schleyer PvR. *Angew. Chem. Int. Ed. Engl.* 1995; **34**: 334–337; (k) Black KA, Wilsey S, Houk KN. *J. Am. Chem. Soc.* 1998; **120**: 5622–5627, and references cited therein.
2. Andersson K, Malmqvist P-Å, Roos BO. *J. Chem. Phys.* 1992; **96**: 1218–1226.
3. Kozlowski PM, Davidson ER. *J. Chem. Phys.* 1994; **100**: 3672–3682.
4. (a) Becke D. *J. Chem. Phys.* 1993; **98**: 5648–5652; (b) Lee C, Yang W, Parr RG. *Phys. Rev. B* 1988; **37**: 785–789.
5. (a) Jiao H, Schleyer PvR. *Angew. Chem. Int. Ed. Engl.* 1995; **34**: 334–337; (b) Jiao H, Nagelkerke R, Kurtz HA, Williams RV, Borden WT, Schleyer PvR. *J. Am. Chem. Soc.* 1997; **119**: 5921–5929.
6. Staroverov VN, Davidson ER. *J. Am. Chem. Soc.* 2000; **122**: 186–187.
7. Roth WR, Hanold F. *Liebigs Ann. Chem.* 1996; 1917–1928.
8. (a) Roth WR, Gleiter R, Paschmann V, Hackler UE, Fritzsche G, Lange H. *Eur. J. Org. Chem.* 1998; **2**: 961–967; (b) Duncan JA, Spong MC. *J. Org. Chem.* 2000; **65**: 5720–5727.
9. (a) Padwa A, Blacklock TJ. *J. Am. Chem. Soc.* 1980; **102**: 2797–2806; (b) Roth WR, Lennartz H-W, Doering WvE, Birladeanu L, Guyton CA, Kitigawa T. *J. Am. Chem. Soc.* 1990; **112**: 1722–1732; (c) Roth WR, Schaffers T, Heiber M. *Chem. Ber.* 1992; **125**: 739–749; (d) Jing N, Lemal DM. *J. Am. Chem. Soc.* 1993; **115**: 8481–8482.
10. Bally T, Borden WT. In *Reviews in Computational Chemistry*, Lipowitz KB, Boyd DB (eds). Wiley: New York, 1999; 38–42.
11. Schreiner PR. *J. Am. Chem. Soc.* 1998; **120**: 4184–4190.
12. Roth WR, Wollweber D, Offerhaus R, Rekowski V, Lennartz H-W, Sustmann R, Müller W. *J. Am. Chem. Soc.* 1994; **116**: 495–505.
13. Wessel TE, Berson JA. *J. Am. Chem. Soc.* 1994; **116**: 495–505.
14. Hrovat DA, Duncan JA, Borden WT. *J. Am. Chem. Soc.* 1999; **121**: 169–175.
15. (a) Duncan JA, Hendricks RT, Kwong KS. *J. Am. Chem. Soc.* 1990; **112**: 8433–8442; (b) Duncan JA. *J. Org. Chem.* 1996; **61**: 4455–4459.
16. Duncan JA, Azar JK, Beathe JC, Kennedy SR, Wulf CM. *J. Am. Chem. Soc.* 1999; **121**: 12029–12034.
17. (a) Frisch MJ, Trucks GW, Schlegel HB, Gill PMW, Johnson BG, Robb MA, Cheeseman JR, Keith T, Petersson GA, Montgomery JA, Raghavachari K, Al-Laham MA, Zakrzewski VG, Ortiz JV, Foresman JB, Cioslowski J, Stefanov BB, Nanayakkara A, Challacombe M, Peng CY, Ayala PY, Chen W, Wong MW, Andres JL, Replogle ES, Gomperts R, Martin R, Fox DJ, Binkley JS, Defrees DJ, Baker J, Stewart JP, Head-Gordon M, Gonzalez C, Pople JA. *Gaussian 94, Revision D4*. Gaussian: Pittsburgh, PA, 1995; (b) Frisch MJ, Trucks GW, Schlegel HB, Scuseria GE, Robb MA, Cheeseman JR, Zakrzewski VG, Montgomery JA, Stratmann RE, Burant JC, Dapprich S, Millam JM, Daniels AD, Kudin KN, Strain MC, Farkas O, Tomasi J, Barone V, Cossi M, Cammi R, Mennucci B, Pomelli C, Adamo C, Clifford S, Ochterski J, Petersson GA, Ayala PY, Cui Q, Morokuma K, Malick DK, Rabuck AD, Raghavachari K, Foresman JB, Cioslowski J, Ortiz JV, Stefanov BB, Liu G, Liashenko A, Piskorz P, Komaromi I, Gomperts R, Martin RL, Fox DJ, Keith T, Al-Laham MA, Peng CY, Nanayakkara A, Gonzalez C, Challacombe M, Gill PMW, Johnson B, Chen W, Wong MW, Andres JL, Head-Gordon M, Replogle ES, Pople JA. *Gaussian 98, Revision A5*. Gaussian: Pittsburgh, PA, 1998.
18. (a) Yamaguchi K, Jensen F, Dorigo A, Houk KN. *Chem. Phys. Lett.* 1988; **149**: 537–542; (b) Yamanaka S, Kawakami T, Nagao H, Yamaguchi K. *Chem. Phys. Lett.* 1994; **231**: 25–33.